

## THE EFFECTS OF WIND ON PLANTS : A REVIEW

Emmanuel de Langre

*Département de Mécanique, LadHyX, Ecole polytechnique, Palaiseau, France*

### ABSTRACT

*This review surveys some of the mechanical interactions between wind and plants, from plant organs to plant systems. The relevant nondimensional parameters are first estimated. Turbulence, plant dynamics and the mechanisms of interaction are discussed in this context. Some common features are identified, and they are analysed in relation with wind-engineering of man-made structures. Strong coupling between plants and wind exist, where the plant motion modifies the wind dynamics. Some related biological issues are also mentioned.*

### 1. INTRODUCTION

The reader is referred to the full version of this review (de Langre, 2008) for : (a) a complete list of relevant references, (b) some details on the issues described below, (c) a description of other topics which are only mentioned in the conclusion.

Some of the earliest work on plant motion under wind goes back to the description of Honamis (Inoue, 1955) which refer to traveling waves on wheat. Since then very abundant literature has been produced on the subject of wind and plants.

Previous surveys such as by Finnigan (2000) have been more focused on the effect of vegetation on wind, in particular on its turbulent features, rather than on the reverse. Many recent reviews exist on specific aspects of the direct or indirect effects of wind on plants, see in (de Langre, 2008). They address the topics of crop dynamics and tree dynamics under wind, seed dispersal by wind, ecological effects of wind, effect of wind on plant growth, or plant evolution under wind constraint. More general concepts may be found in the earlier reviews of Mayer (1987) and Vangardingén & Grace (1991), as well as in the essential book on plant biomechanics by Niklas (1992).

### 2. NONDIMENSIONAL NUMBERS

In view of the immense variety of possible interactions a preliminary dimensional analysis appears

necessary. In addition to the parameters related to wind and to plant dynamics considered separately, there exist nondimensional parameters pertaining to the interactions. They may be derived by elementary dimensional analysis. For a reference wind velocity  $U$  and density  $\rho_F$ , using the modulus of elasticity  $E$  and density  $\rho_S$  for the solid, two nondimensional parameters arise

$$\mathcal{M} = \frac{\rho_F}{\rho_S}, \quad C_Y = \frac{\rho_F U^2}{E}, \quad (1)$$

which are respectively the mass ratio and the Cauchy number, commonly used in the mechanics of fluid-structure interactions.

The mass ratio is of the order of  $10^{-3}$  for all case of wind plant interactions, the density of vegetal material being typically  $10^3$  higher than air. As  $\mathcal{M}$  scales the added mass caused by the fluid motion resulting from the solid motion, this inertial effect is usually negligible, except for some plane structures such as leaves where geometry effects play a central role.

The Cauchy number  $C_Y$ , which scales the deformation of an elastic solid under the effect of flow, is defined as the ratio of the dynamic pressure and the modulus of elasticity. For a modulus of  $10^8$  Pa, corresponding to soft living vegetal tissues and for a wind velocity of 10 m/s, corresponding to very high wind conditions at a plant level, the Cauchy number is of order  $10^{-6}$ . As this would imply that no deformation can be expected in the plant, it is clearly inappropriate, common knowledge showing strong deflections in plants. In fact the slenderness of plants need to be taken into account in the deformability: most vegetal structures are slender in order to access light and carbon. A slenderness number  $\mathcal{S}$  therefore needs to be defined as the ratio of the maximum to minimum cross-sectional dimensions of the system  $L$  and  $\ell$  respectively. The deformation of a slender beam in bending under a transverse surface load being proportional to  $\mathcal{S}^3$ , (Niklas, 1992), the convenient set of dimensionless num-

bers now reads

$$\mathcal{M} = \frac{\rho_F}{\rho_S}, \mathcal{S} = \frac{L}{\ell}, C_Y = \frac{\rho_F U^2 L^3}{E \ell^3} = \frac{\rho_F U^2}{E} \mathcal{S}^3. \quad (2)$$

Figure 1a illustrates the influence of the slenderness on the order of magnitude of the Cauchy number. As a slenderness of more than 100 is not uncommon in stems a Cauchy number of order unity may be expected for a wind of 10 m/s. Therefore, in contrast to most structures encountered in classical wind engineering, where the slenderness may also be large (antennas, cables) but where the stiffness is usually of two orders of magnitudes larger, a significant static deformation of a plant can be expected under the action of wind. This is an important specificity of wind effect on plants.

The reduced velocity, denoted  $U_R$ , may be defined as the ratio of the period of free vibration of the solid,  $T$ , over the advection time across the solid, here  $\ell/U$ . Considering that the period of oscillation of a slender beam scales as  $(L^2/\ell)\sqrt{\rho_S/E}$  the reduced velocity is easily expressed using the preceding numbers as  $U_R^2 = C_Y \mathcal{S}/\mathcal{M}$ . When the reduced velocity is of order unity dynamical interactions, such as resonances or lock-in, may be expected as the two time scales become close. As illustrated in Figure 1b this may happen in a large range of wind velocities and plant slenderness.

### 3. WIND IN THE PRESENCE OF PLANTS

The presence of plants affects the characteristics of wind, so that data used in wind engineering for man-made structures are often inappropriate for plants. The review by Finnigan (2000) fully documents flow and turbulence at the scale of the plant canopy itself. See also some recent numerical work, such as in (Dupont & Brunet, 2008).

In the absence of vegetation, the distribution of time-averaged wind horizontal velocity is logarithmic, Figure 2a. In a canopy, wind exists, in the form of an inner boundary layer, Figure 2b. This flow profile then connects to the outer boundary layer above the canopy. It will now be referred to as the Canopy Layer as opposed to the Boundary Layer profile. In terms of turbulence characteristics the Canopy Layer case displays strong differences with the Boundary Layer. In the latter, fully developed turbulence results in the classical Kolmogorov cascade from large to small scales, sketched in Figure 2a. The corresponding spectrum of horizontal fluctuating ve-

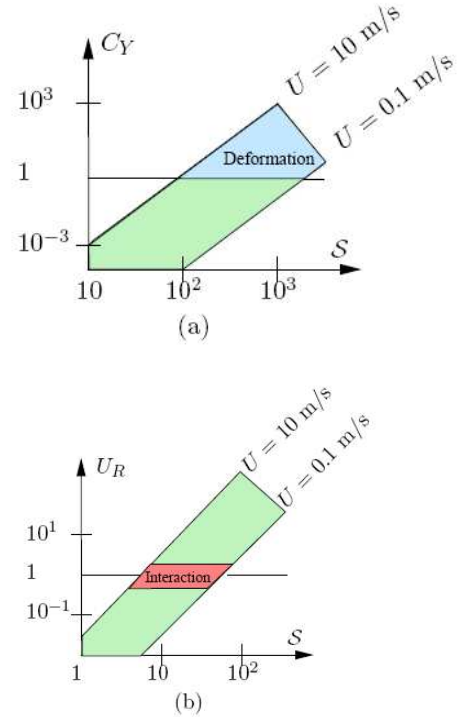


Figure 1: Effect of slenderness on dimensionless numbers relevant to wind effects on plants. (a) The Cauchy number may exceed one, which corresponds to large plant deformation. (b) The reduced velocity may become of order one, which corresponds to strong dynamical coupling.

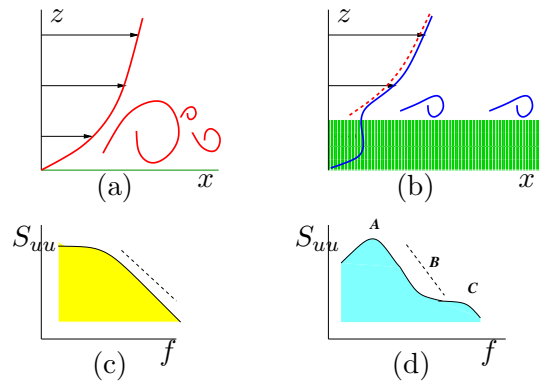


Figure 2: Main differences between Boundary Layer flow (a,c) and Canopy Layer flow (b,d). Top: Wind profile and structure of eddies. Bottom: Spectrum of fluctuations of the horizontal velocity,  $S_{uu}$ . See text for features corresponding to **A**, **B**, **C**.

locity, is shown in Figure 2c. Conversely, in the Canopy Layer, fluctuations are mainly generated by a mixing layer instability that develops from the inflectional wind profile, Figure 2b. This results in large coherent structures being convected above the canopy. The corresponding Canopy Layer velocity spectrum, Figure 2d, differs from the Boundary Layer spectrum by three aspects. First, it shows a more pronounced peak at a central frequency which is that of the mixing layer instability (labeled **A** in the figure). Second, because of the drag on all elements of plants in the canopy the dissipation cascade is enhanced, showing a steeper decrease with frequency (**B** in the figure). Finally this interaction with the plants, as well as the possible swaying of branches or leaves cause the emission of vortices at higher frequencies, resulting in a possible second peak in the spectrum (**C**).

#### 4. WIND LOAD AND PLANT RESPONSE

The interactions of wind and plant dynamics may be described in the framework of modal analysis. Models such as in Wood (1995); Baker (1995); Saunderson *et al.* (1999); Kerzenmacher & Gardiner (1998); Spatz & Bruechert (2000) may be seen as particular cases of this approach.

##### 4.1. Drag on plants

Wind on plant surface causes local skin friction and pressure drag. The net drag load on a plant, or on part of a plant, may be measured in a wind tunnel with a load cell. Depending on the scale of interest, the plant or subsets of the plant may be regarded either as a bluff body surrounded by air-flow such as an individual leaf, or as a porous body with through-flow such as a tree crown, as discussed in Section 4.2 when introducing the concept of porosity. In the first case a drag load is commonly expressed as

$$\mathbf{F} = \frac{1}{2}\rho AC_D |\mathbf{U} - \dot{\mathbf{X}}|(\mathbf{U} - \dot{\mathbf{X}}), \quad (3)$$

where the drag factor  $AC_D$  depends on the geometry and the Reynolds number. Note that we shall not separate here the reference area  $A$  and the drag coefficient  $C_D$ , as only their combined effect matters. The dependence of the drag coefficient on wind-induced change in plant configuration will be discussed in Section 6. Using equation (3) with a time varying wind velocity  $\mathbf{U}$  and

plant velocity  $\dot{\mathbf{X}}$  allows to derive a time varying load  $\mathbf{F}$ . Alternatively when using a porous medium model a local volume drag load may also be defined as

$$\mathbf{f} = \frac{1}{2}\rho\epsilon c_D |\mathbf{U} - \dot{\mathbf{X}}|(\mathbf{U} - \dot{\mathbf{X}}). \quad (4)$$

In a canopy, the combined drag coefficient  $\epsilon c_D$  essentially varies with  $z$  and may be derived from the variation of the Reynolds stress  $\epsilon c_D = \overline{(u'w')}_z / u^2$  (Kerzenmacher & Gardiner, 1998). The drag coefficient  $c_D$  is found to be of the order of 0.1 for trees. Note that a point load, as defined by equation (3), may be considered as a particular volume distributed load given by equation (4), so that only this case will be mentioned further.

From this local definition of wind load over the porous media the modal wind load for mode  $n$  is easily derived by a modal projection integrating over the whole volume

$$f_n = \int \mathbf{f} \cdot \boldsymbol{\varphi}_n \, d\Omega. \quad (5)$$

Elementary cases of interest are easily recovered by choosing specific forms of the modal shape: the net drag upon using a translational mode  $\boldsymbol{\varphi} = \underline{e}_X$ , the moment on root plate with  $\boldsymbol{\varphi} = (z/L)\underline{e}_X$  and the torsional load using  $\boldsymbol{\varphi} = r\underline{e}_\theta$  in cylindrical coordinates.

##### 4.2. Modal response

The dynamics of a given mode  $n$  excited by wind is then defined by

$$m\ddot{q} + c\dot{q} + kq = \int \frac{1}{2}\rho\epsilon c_D |\mathbf{U} - \dot{q}\boldsymbol{\varphi}|(\mathbf{U} - \dot{q}\boldsymbol{\varphi}) \cdot \boldsymbol{\varphi} \, d\Omega. \quad (6)$$

Upon removing all time dependent terms the static contribution of each mode may thus be derived, and the total static response as well by superposition. For each mode, damping in still air and flow-induced damping are also found by assuming  $\mathbf{U} = 0$  or  $\dot{q} \ll |U|$  respectively. Another important case arises when the wind velocity fluctuations are taken into account. The fluctuations  $u$  such that  $U(t) = U + u(t)$  are known only through their spectral characteristics, such as  $S_{uu}$ , as described in Section 3. In that case, the plant velocities are usually considered to be of smaller amplitude so that the load does not depend on  $\dot{q}$ . When fluctuations are assumed to be small  $u^2$  terms may be neglected versus  $Uu$  terms, and the general framework of linear spectral analysis may be applied.

The methodology to derive the spectral characteristics of the response, such as the Power Spectral Density (PSD) of displacement at a given point, from the spectral characteristics of wind is then a standard procedure as in the prediction of turbulence-induced vibrations in hydrodynamics and in wind-engineering. Specific features exist in the case of wind over plants (Mayer, 1987; Gardiner, 1995; Baker, 1995). First, the aerodynamic admittance is usually close to unity, as wind load are strongly correlated over a plant. This results from the comparison of the plant size,  $L$  to the size of eddies that contribute to the excitation. Second, by contrast to the large structures of interest in wind engineering, such as bridges or antennas, damping is high and modes may be close to each other which may not allow standard simplifications in the combination of modal responses. Finally the large deformability of plants causes large amplitudes of motion, so that non-linear effects due to geometry or contact with other plants such as crown clashing in trees, may come into play. In such cases, the equation of motion may also be solved using modes but in the time-domain, via a standard procedure in flow-induced vibrations.

### 4.3. Propagating load on canopies

As mentioned in Section 3 the low frequency content of the wind spectra is associated to propagating gusts over a canopy resulting from a mixing layer instability. If one considers the response of a given plant, the spectral description presented above for the modal response is adequate, as propagating gusts are simply seen as low frequency events. The global response of the canopy may also be sought, where load varies both in space and time. The spectral procedure is still applicable to propagating loads, through the use of complex correlation functions to derive the modal admittances. Alternatively a simple model where the load is time-independent in a moving frame of reference may be used, (Farquhar & Eggleton, 2000; Doaré *et al.*, 2004). In such a frame defined by  $X = x - Ut$  the modal equation for the canopy reads

$$(mU^2 - r)q'' - cUq' + kq = f(X) \quad (7)$$

where primes are derivatives with respect to  $X$ . The dependence in space is then equivalent to the time dependence of an oscillator: resonance conditions may occur for specific wavelengths of the gust. Moreover, the motion of the canopy behind a step gust resembles the evolution of a damped

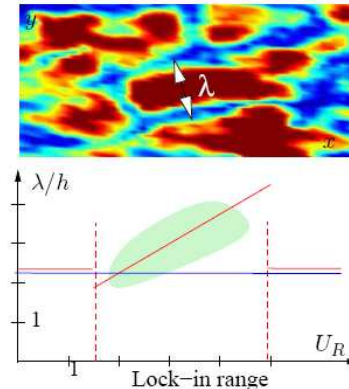


Figure 3: Honami lock-in, scaled by the reduced velocity (Py *et al.*, 2006). Top: Experimental data of the instantaneous velocity magnitude of plants on an alfalfa field under wind displaying a wavelength  $\lambda$ . Bottom: Comparison between experimental data on alfalfa (green zone) and theoretical prediction of a wavelength lock-in effect, in red, using the coupled model. The simple mixing layer model, in blue, fails to capture this effect.

oscillator, where the time variable is replaced by  $-X$ . Non-linear effects due to the interactions between plants are easily taken into account, see Doaré *et al.* (2004).

## 5. FULLY COUPLED MODELS OF WIND-PLANT INTERACTIONS

### 5.1. Honami lock-in: a Reduced Velocity effect

As described above a mixing layer instability develops above a canopy, creating large scale coherent fluctuations. The most amplified wavelength is classically derived by a linear temporal stability analysis of the inflectional velocity profile and scales with the mixing layer thickness. A more refined linear stability analysis is possible including both the flow and the flexible canopy, as in the recent study of Py *et al.* (2006). In such a model, the drag resulting from flow fluctuation affects the canopy dynamics and is simultaneously incorporated in the linearized momentum equation. The temporal stability analysis associated with these coupled equations shows a surprising lock-in feature in a specific range of flow velocities: the wavelength of the instability no longer scales with the mixing layer thickness, Figure 3. This range is defined by a reduced velocity  $U_R$  of order unity. The wavelength then scales with  $U_R$ ,

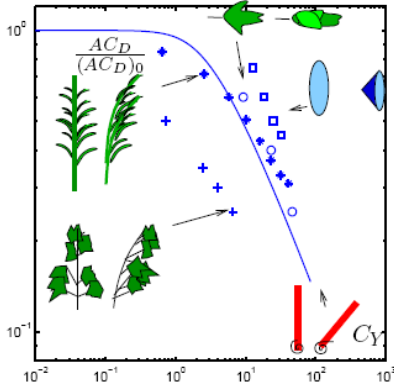


Figure 4: Reconfiguration: variation of the drag factor with the Cauchy number. Blue line: model of a cylinder mounted on a rotational spring. (+) maple tree crown, (\*) giant reed, (o) tulip tree leaf,  $\square$  flexible sheet. See text for reference.

as the frequency of the instability locks on the frequency of the canopy. Experimental data of honamis on wheat fields and alfalfa fields confirm this effect (Py *et al.*, 2006).

## 5.2. Drag reduction: a Cauchy number effect

The preceding lock-in phenomenon is linear by nature. Coupling also arises through nonlinearities, when the body shape change needs to be of order unity to affect the wind load. The drag induced by wind has here been assumed to vary as  $F = \rho U^2 AC_D/2$ . It has often been reported that the  $U^2$  variation of drag did not apply for plants. This has been expressed in terms of a "Vogel exponent" noted  $b$  such that the dependence of drag load with velocity scales as  $U^{2+b}$ . A value of  $b = -1$  is not uncommon, so that the drag load increases linearly with the velocity. Some Reynolds number effects may be the cause for the smallest plant components, but most observations relate this reduction to significant deformations of the plant. Such shape change may take different forms, from a simple pronounced bending to wrapping, and they fall under the generic name of reconfiguration (Vogel, 1989). It is an essential mechanism by which vegetation reduce stress induced by external flow, in air or water, see Harder *et al.* (2004). According to the dimensional analysis it is expected to depend on the Cauchy number, which controls the shape changes of the plant due to flow. For a non-porous body, as defined in Section 4, flow-induced

deformation may affect drag through two distinct mechanisms. First, as noted by most authors, deformation induces a reduction in the effective cross flow area,  $A$ , which does directly reduce the total drag load. Second the deformed shape may be more streamlined so that the pressure recovery in its wake is improved, also reducing drag. These combined effects are fully discussed by Alben *et al.* (2004) for the model case of a thread in a soap film, a 2D model for fluid flow, and by Vollsinger *et al.* (2005) for a tree crown in a wind tunnel: they are found to be of similar magnitude. Figure 4 shows typical experimental data of the evolution of the drag reduction ratio  $AC_D/(AC_D)_0$  with Cauchy number, see (de Langre, 2008) for details on references. All these evolutions display a strong decrease of drag for a Cauchy number of order unity.

As an elementary model of this effect one may consider a rigid cylinder of length  $L$  and diameter  $D$  mounted on a rotational spring of stiffness  $C$ , which allows deformation by bending in the flow direction, Figure 4. Assuming that the drag depends on the velocity normal to the cylinder, the drag reduction ratio varies as  $AC_D/(AC_D)_0 = \cos^2 \theta$ , where  $\theta$  is the angle of inclination. Using the equilibrium of moments between drag and rotational stiffness yields  $C_Y = \rho U^2 D/C = 4\theta/\cos^3 \theta$ . The relation between drag and Cauchy number using this model is shown in Figure 4. It is found to qualitatively represent the reconfiguration effect observed in the experimental data.

## 6. CONCLUDING REMARKS

Though the effects of wind on plants are manifold, even in the restricted context of mechanics, several common features may be identified. First, the fluid mechanics of wind in the presence of plant and the solid mechanics of plants are themselves quite specific: wind turbulence is different from its counterpart in classical boundary layers, and plant structural dynamics is different from its counterpart in man-made structures. Second, the interactions that cause motion of plants or of part of plants are caused by mechanisms that are well-known in flow-induced vibration, but several important specific features raise challenging questions: the range of length scales in a given medium (from leaves to canopies), the complex three-dimensional geometries (from individual plant architecture to seed dispersal in a rainforest) and the magnitude of deformation (from fluttering leaf to streamlined tree crown).

Other important effect of wind of plants must be mentioned, see in (de Langre, 2008). First, wind strongly affects photosynthesis, by its effects on the thermal boundary layer, but also by the role of leaf motion in light perception. Wind is also an essential ingredient of several biological functions through its role in seed dispersal, windthrow and thigmomorphogenesis. Finally, wind affects the interactions between plants and animals, such as insect communication

*Acknowledgment* : Financial support of the French ANR program "CHENE-ROSEAU", involving INRA, INRIA and Ecole polytechnique is gratefully acknowledged.

## 7. REFERENCES

- ALBEN, S., SHELLEY, M. & ZHANG, J. 2004 How flexibility induces streamlining in a two-dimensional flow. *Physics of Fluids* **16** (5), 1694 – 1713.
- BAKER, C. 1995 The development of a theoretical model for the windthrow of plants. *Journal of Theoretical Biology* **175** (3), 355–372.
- DOARÉ, O., MOULIA, B. & DE LANGRE, E. 2004 Effect of plant interaction on wind-induced crop motion. *Journal of Biomechanical Engineering* **126** (2), 146 – 151.
- DUPONT, S. & BRUNET, Y. 2008 Edge Flow and Canopy Structure: A Large-Eddy Simulation Study. *Boundary-Layer Meteorology* **126** (1), 51–71.
- FARQUHAR, T. & EGGLETON, C. 2000 Pulsatile flow heightens vertical exchanges in a wheat canopy. *Proceedings of the 3rd Plant Biomechanics Conference, Freiburg, Spatz, HC and Speck, Th. Eds* .
- FINNIGAN, J. 2000 Turbulence in Plant Canopies. *Annual Review of Fluid Mechanics* **32** (1), 519–571.
- GARDINER, B. A. 1995 The interactions of wind and tree movement in forest canopies. In *Wind and trees*. Cambridge: Cambridge University Press.
- HARDER, D. L., SPECK, O., HURD, C. L. & SPECK, T. 2004 Reconfiguration as a prerequisite for survival in highly unstable flow-dominated habitats. *Journal of Plant Growth Regulation* **23** (2), 98 – 107.
- INOUE, E. 1955 Studies of the phenomena of waving plants (HONAMI) caused by wind. Part 1. Mechanism and characteristics of waving plants phenomena. *J. Agric. Meteorol.(Japan)* **11**, 18–22.
- KERZENMACHER, T. & GARDINER, B. 1998 A mathematical model to describe the dynamic response of a spruce tree to the wind. *Trees-Structure and Function* **12** (6), 385–394.
- DE LANGRE, E. 2008 Effects of Wind on Plants. *Annual Review of Fluid Mechanics* **40** (1), 141–168.
- MAYER, H. 1987 Wind-induced tree sways. *Trees-Structure and Function* **1** (4), 195–206.
- NIKLAS, K. 1992 *Plant Biomechanics: An Engineering Approach to Plant Form and Function*. University of Chicago Press.
- PY, C., DE LANGRE, E. & MOULIA, B. 2006 A frequency lock-in mechanism in the interaction between wind and crop canopies. *Journal of Fluid Mechanics* **568**, 425–449.
- SAUNDERSON, S., ENGLAND, A. & BAKER, C. 1999 A dynamic model of the behaviour of sitka spruce in high winds. *Journal of Theoretical Biology* **200** (3), 249 – 259.
- SPATZ, H. C. & BRUECHERT, F. 2000 Basic biomechanics of self-supporting plants: wind loads and gravitational loads on a norway spruce tree. *Forest Ecology and Management* **135** (1-3), 33 – 44.
- VANGARDINGEN, P. & GRACE, J. 1991 Plants and wind. *Advances in Botanical Research Incorporating advances in Plant Pathology* **18**, 189 – 253.
- VOGEL, S. 1989 Drag and reconfiguration of broad leaves in high winds. *Journal of Experimental Botany* **40** (217), 941 – 948.
- VOLLSINGER, S., MITCHELL, S. J., BYRNE, K. E., NOVAK, M. D. & RUDNICKI, M. 2005 Wind tunnel measurements of crown streamlining and drag relationships for several hardwood species. *Canadian Journal of Forest Research* **35** (5), 1238 – 1249.
- WOOD, C. 1995 Understanding wind forces on trees. In *Wind and Trees*. Cambridge: Cambridge University Press.